

## Metal Binding and Selectivity in Zinc Proteins

Todor Dudev<sup>a,\*</sup> (杜 鐸) and Carmay Lim<sup>a,b,\*</sup> (林小喬)

<sup>a</sup>*Institute of Biomedical Sciences, Academia Sinica, Taipei 11529, Taiwan, R.O.C.*

<sup>b</sup>*Department of Chemistry, National Tsing Hua University, Hsinchu 300, Taiwan, R.O.C.*

Zinc is one of the most abundant metals in living organisms and is an essential co-factor of many metabolic enzymes and transcription factors. In this review, based on a recent body of theoretical and experimental results, the physical bases are delineated for the following aspects of zinc binding and selectivity in proteins: (1) What is the most thermodynamically preferable coordination geometry of a bidentate ligand (such as carboxylate) or Zn in Zn-binding sites? (2) What is the protonation state of the Cys side chain in Cys<sub>4</sub> zinc-finger cores? (3) How does a protein select Zn from the mixture of ions in the surrounding fluids? (4) What is the role of the second shell in metal binding and selectivity? The key results are summarized and the physical basis and/or implications of the findings are discussed.

**Keywords:** Zinc; Zn; Metal binding; Metal selectivity; Second shell; Coordination geometry.

### INTRODUCTION

Almost half of all known proteins contain metal co-factor(s).<sup>1</sup> Metals perform a variety of tasks ranging from protein structure stabilization to enzyme catalysis, activating many essential life processes such as respiration and photosynthesis.<sup>2-5</sup> Among the metals, Na, K, Mg, Ca, Zn, Cu, Fe, Co, and Mn are most frequently found to bind to proteins under physiological conditions.<sup>2,4</sup> These metals tend to bind directly to a shell of polar hydrophilic residues (inner-sphere mode) surrounded by a shell of non-polar hydrophobic groups.<sup>6,7</sup> Here, we focus on Zn(II), the second most abundant transition metal in humans (2.3 g of Zn for an average person<sup>8</sup>) as well as in seawater because it has been well studied not only experimentally but also theoretically. Based on this body of computational and experimental results, we attempt to delineate some fundamental principles governing Zn(II) binding and selectivity in proteins. In what follows, we first summarize the known biological roles of Zn, sequence motifs and/or structural characteristics of Zn-binding sites, and Zn coordination chemistry before presenting the specific questions that are addressed in this review.

Zinc is an essential co-factor of many metabolic enzymes and transcription factors.<sup>5,9-12</sup> In general, Zn-binding sites in proteins can be divided into two categories: (1) sites that play predominantly a catalytic role ("catalytic" Zn-sites) and (2) sites that serve only a structural role ("structural" Zn-sites). The most common Zn-chelating sphere found in

the first category is His<sub>3</sub>Water, although catalytic sites containing < 3 His, Asp/Glu or Cys side chains have also been observed.<sup>9,11,13,14</sup> The best studied "structural" Zn-proteins are those of the Zn-finger family, which is involved in nucleic acid binding and gene regulation.<sup>11,15</sup> Commonly accepted classes of Zn-fingers include: (a) the cellular or transcription factor type, characterized by a Cys<sub>2</sub>His<sub>2</sub> metal-binding site;<sup>16,17</sup> (b) the retroviral type, possessing a Cys<sub>3</sub>His chelation sphere,<sup>18</sup> and (c) the steroid receptor type, having a Cys<sub>4</sub> metal-binding site.<sup>19</sup> In contrast to the "catalytic" Zn-sites, which are partially exposed to solvent, the "structural" Zn-sites are fully/partially buried and are surrounded by an elaborate network of hydrogen bonds from the second layer.<sup>20</sup>

Zn prefers "soft" ligands like Cys and His, but it is also found coordinated to Asp and Glu side chains.<sup>21-23</sup> In aqueous solution Zn is octahedrally bound to six water molecules with an average Zn-O(Water) distance of 2.10 Å.<sup>24</sup> In proteins, however, Zn is usually tetrahedrally coordinated, but it can also adopt a 5- or 6-coordinate geometry in some enzymes. The average Zn-ligand bond distances for a tetrahedral binding site are (in Å): Zn-N(His) 2.07-2.09; Zn-S(Cys) 2.21-2.35; Zn-O(Asp/Glu) 1.95-2.04; Zn-O(Water) 2.12-2.15.<sup>13</sup>

Although a wealth of information has been accumulated on the biochemical and physiological significance of Zn, no generic rules on its binding and selectivity in proteins has been reported (to the best of our knowledge). Here, based on findings from our group and other research groups, we de-

\* Corresponding authors. Tel: +886-2-27899043; fax: +886-2-27887641; e-mail: carmay@gate.sinica.edu.tw; todor@ibms.sinica.edu.tw

lineate the physical bases for the following aspects of zinc binding and selectivity in proteins (1) What is the most thermodynamically preferable coordination geometry of a bidentate ligand (such as carboxylate) or Zn in Zn-binding sites? (2) What is the protonation state of the Cys side chain in Cys<sub>4</sub> zinc-finger cores? (3) What is the role of the second shell in metal binding and selectivity? (4) How does a protein select Zn from the mixture of ions in the surrounding fluids? In each of the following sections, we first present the background/rationale and outline the approach (depending on the original references to provide details of the methodology/computations). Then, the key results are summarized and the physical basis and/or implications of the findings are discussed.

### A. The mode of carboxylate binding (mono- or bidentate) in Zn complexes depends on other interactions within the complex

Catalytic binding sites in Zn-enzymes often contain Asp or Glu.<sup>12,21-23</sup> The carboxylate side-chains generally bind to Zn in either monodentate or bidentate fashion with an average Zn-O distance around 1.8-2.0 Å and 2.1-2.4 Å, respectively. In some proteins (e.g., bacillolysine and sonic hedgehog) they bind to the metal in an intermediate mode that is neither monodentate nor bidentate, as manifested by Zn-O bond distances around 2.0-2.1 Å and 2.5-2.8 Å.<sup>12</sup> To elucidate the factors determining the carboxylate coordination mode to Zn, the relative energies for Zn tetrahedrally bound to various CH<sub>3</sub>COO<sup>-</sup> (Ace) coordination modes, OH<sup>-</sup>, imidazole (Im), and H<sub>2</sub>O have been calculated using density functional theory (see Fig. 1).<sup>25</sup> These Zn complexes model metal-binding sites in Zn-enzymes such as carboxypeptidase and thermolysin.

Fig. 1 shows the most favorable acetate coordination mode and relative energies for tetrahedral Zn complexes with H<sub>2</sub>O, OH<sup>-</sup>, imidazole, and CH<sub>3</sub>COO<sup>-</sup>. For complexes with only inner-shell ligands, *monodentate* carboxylate binding is preferred except for [Zn Im<sub>3</sub> Ace]<sup>+</sup>, which prefers an intermediate mode to isoenergetic mono-/bi-dentate binding.<sup>25</sup> Including second-shell water molecule(s) reverses the trend for the [Zn Im<sub>2</sub> Ace H<sub>2</sub>O] complex due to favorable inter-ligand interactions, which favor the *bidentate* mode (Fig. 1D).

These results imply that the carboxylate coordination mode to Zn is governed *not* by the carboxylate group itself, but by other interactions within the complex. They also highlight the crucial role of hydrogen bonds among inner-shell ligands, and between inner and outer shell ligands in stabilizing the metal-binding site structure.<sup>25</sup> Since the energy barrier for switching between mono- and bi-dentate coordination is calculated to be only a few kcal/mol,<sup>25</sup> the protein may

adopt a functional binding site configuration at a relatively low energy cost.

### B. Tetrahedral Zn complexes in protein cavities are more stable than other zinc polyhedra

Mg(II), with an ionic radius (0.72 Å) similar to that of Zn(II) (0.75 Å), is usually octahedrally coordinated both in aqueous solution and in proteins.<sup>26</sup> Zn, however, is flexible with respect to the number of first-shell ligands in proteins. In "structural" Zn-sites, Zn is found to be *tetrahedrally* coordinated, whereas in "catalytic" Zn-sites it is found to be both *tetrahedrally* and *penta*-coordinated and, rarely, hexacoordinated (the ratio between 4:5:6-coordinate zinc is 62:36:2%).<sup>23</sup> To elucidate the lowest-energy, ground state coordination geometry for Zn complexes in proteins, the free energies of

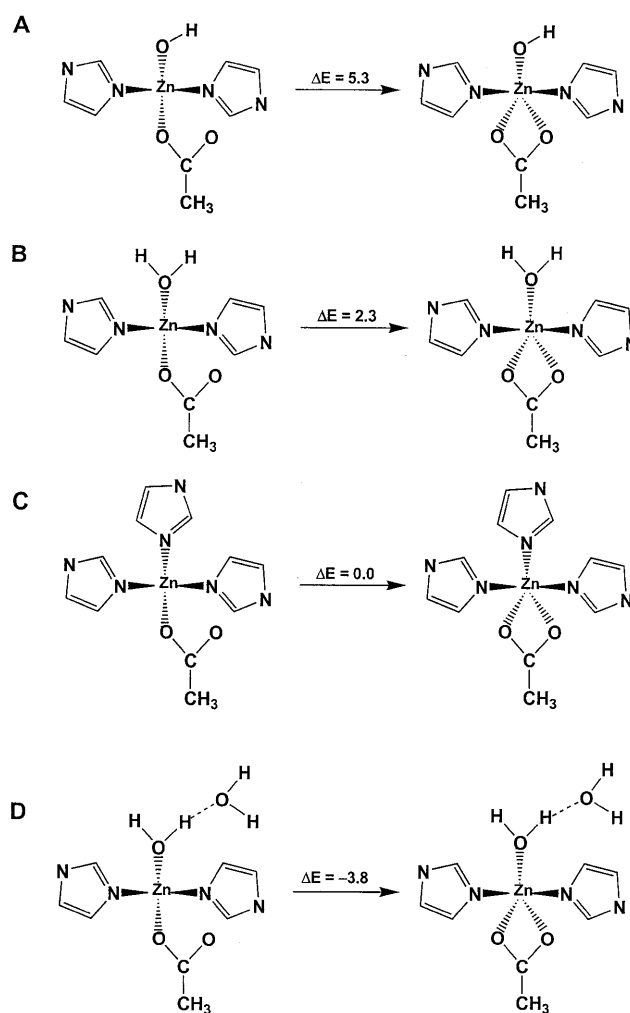


Fig. 1. Schematic diagrams of Zn tetrahedrally bound to mono- and bi-dentate CH<sub>3</sub>COO<sup>-</sup>, OH<sup>-</sup>, imidazole and H<sub>2</sub>O. The relative energies (in kcal/mol) are taken from Ryde, 1999.<sup>25</sup>

Table 1. Calculated Enthalpies ( $\Delta H_{\text{isom}}^1$ ) and Free Energies of Isomerization ( $\Delta G_{\text{isom}}^x$ ) between Octahedral and Tetrahedral Zn and Mg Complexes for Media of Different Dielectric Constant  $x$  (in kcal/mol)<sup>a</sup>

Reaction	$\Delta H_{\text{isom}}^{1,b}$	$\Delta G_{\text{isom}}^1$	$\Delta G_{\text{isom}}^2$	$\Delta G_{\text{isom}}^4$	$\Delta G_{\text{isom}}^{80}$
$[\text{Zn W}_6]^{2+} \leftrightarrow ([\text{Zn W}_4] \cdot \text{W}_2)^{2+}$	-2.3	-3.7	1.0	3.4	6.8
$[\text{Zn W}_5 \text{ Im}]^{2+} \leftrightarrow ([\text{Zn W}_3 \text{ Im}] \cdot \text{W}_2)^{2+}$	-8.2	-8.4	-3.1	-0.4	2.7
$[\text{Zn W}_4 \text{ Im}_2]^{2+} \leftrightarrow ([\text{Zn W}_2 \text{ Im}_2] \cdot \text{W}_2)^{2+}$	-12.9	-13.9	-8.1	-5.3	-3.7
$[\text{Zn W}_5 \text{ HCOO}]^+ \leftrightarrow ([\text{Zn W}_3 \text{ HCOO}] \cdot \text{W}_2)^+$	-5.4	-9.6	-8.1	-7.3	-6.3
$[\text{Mg W}_6]^{2+} \leftrightarrow ([\text{Mg W}_4] \cdot \text{W}_2)^{2+}$	5.3	4.3	9.6	12.3	15.5
$[\text{Mg W}_5 \text{ Im}]^{2+} \leftrightarrow ([\text{Mg W}_3 \text{ Im}] \cdot \text{W}_2)^{2+}$	1.2	1.7	6.8	9.4	12.4
$[\text{Mg W}_5 \text{ HCOO}]^+ \leftrightarrow ([\text{Mg W}_3 \text{ HCOO}] \cdot \text{W}_2)^+$	7.2	3.1	4.9	5.9	7.0

<sup>a</sup> From Dudev & Lim, 2000;<sup>27</sup>  $x = 1$  corresponds to gas-phase values,  $x = 2$  or 4 represents buried or partially buried metal-binding sites, whereas  $x = 80$  represents fully solvent-exposed sites. <sup>b</sup> Evaluated by B3LYP/6-31++G(2d,2p) calculations using fully optimized B3LYP/6-31++G(2d,2p) molecular geometries.<sup>27</sup>

isomerization between octahedral  $[\text{Zn W}_n \text{ L}_{6-n}]^{2+}$  ( $n = 4, 5, 6$ ) complexes with six ligands in the first shell, and tetrahedral  $([\text{Zn W}_n \text{ L}_{4-n}] \cdot \text{W}_2)^{2+}$  ( $n = 2, 3, 4$ ) complexes with four ligands in the first shell and two water molecules in the second shell have been computed for various dielectric media using density functional theory and continuum dielectric methods (DFT/CDM). These values are compared with the corresponding free energies of isomerization between octahedral and tetrahedral Mg complexes in Table 1.<sup>27</sup>

In a *protein* environment, Zn can adopt octahedral or tetrahedral geometry depending on (i) the type of protein ligand it is bound to and (ii) the solvent accessibility of the metal-binding site.<sup>27</sup> For Zn complexes containing a *neutral* imidazole (representing the His side-chain), tetrahedral geometry is preferred if the binding site is buried ( $\epsilon \leq 4$ ), but both tetrahedral and octahedral structures may exist if the site is solvent accessible ( $\epsilon > 4$ , see Table 1). For Zn complexes containing two imidazoles or a *negatively charged* formate, tetrahedral coordination is favored over octahedral coordination in both buried and solvent-exposed binding sites (negative  $\Delta G_{\text{isom}}$  for reactions 3 and 4 in Table 1). *Tetra-coordinated* Zn structures have also been found to be more stable than the respective penta-coordinated species by 24-48 kcal/mol in the alcohol dehydrogenase active site.<sup>28,29</sup> Furthermore, the 4-coordinate Zn structures have shorter metal-ligand distances than the respective 5- or 6-coordinate all-inner-sphere structures. In contrast to Zn, Mg prefers to be octahedrally coordinated to an imidazole or a formate in both buried and solvent-exposed binding sites (positive  $\Delta G_{\text{isom}}$  for the last two reactions in Table 1).

Three factors favor Zn to be tetra-coordinated. The first is a solvent-inaccessible, low dielectric medium, as evidenced by the greater stability of the tetrahedral Zn hydrate relative to the octahedral one in the gas phase (by -3.7 kcal/mol, Table 1). The second is the charge transfer from the

ligand(s) to the metal cation. The amino acid side-chains, being more polarizable than water, transfer more charge than water to Zn, resulting in a greater neutralization of the positive charge on Zn, which reduces charge-charge and/or charge-dipole interactions.<sup>27</sup> The low positive charge on *penta-* and *hexa-*coordinated Zn, and electron repulsion among the protein ligands would disfavor binding of water molecule(s) in the inner sphere compared to that in the outer sphere. The third is the availability of vacant (hybridized 3d4s) Zn orbitals, close in energy to the highest occupied orbital, which can accept charge from the ligands. In contrast, the vacant (3s) Mg orbitals are much higher in energy than the highest occupied orbital, and cannot accept as much ligand charge as the hybridized 3d4s Zn orbitals. Hence, for a given set of protein ligands, the positive charge on Mg is not as neutralized as that on Zn, thus Mg can remain octahedrally coordinated in proteins as in aqueous solution.

The finding that in protein cavities *4-coordinated* Zn is relatively more stable than 4- or 6-coordinated Zn has two implications. First, tetrahedral Zn-binding sites do not significantly contribute "coordination strain" to the catalytic activity of Zn enzymes.<sup>27</sup> Second, tetrahedral Zn-binding sites with shorter metal-ligand bond lengths are well suited for stabilizing a given protein fold. This is in accord with the fact that all structural mononuclear Zn-binding sites found to date are tetrahedrally coordinated.<sup>11,13,30</sup>

### C. Cys side chains in zinc-finger cores are deprotonated upon metal binding on solvent-exposed surfaces and would not be reprotonated if the binding site is encapsulated by second-shell backbone groups or Lys/Arg side chains

Cys is the most preferred inner-shell ligand for Zn.<sup>23</sup> At physiological pH, Cys side chains with typical  $\text{pK}_a$  values between 8 and 9<sup>31,32</sup> would be protonated in metal-free proteins.

Binding to Zn (acting as a Lewis acid) lowers the Cys pK<sub>a</sub>,<sup>33</sup> thus facilitating sulfhydryl group deprotonation under physiological conditions. However, it is not clear if the zinc cation, with its positive charge reduced by charge transfer from the first two bound cysteines, could still assist deprotonation of the next one or two Cys in Cys<sub>3</sub>His and Cys<sub>4</sub> zinc-finger cores. To elucidate the factors governing the Cys protonation state in Zn·Cys<sub>4</sub> complexes,<sup>30</sup> the free energies for the successive deprotonation of H<sub>2</sub>S in a model steroid receptor-binding site, Zn(H<sub>2</sub>S)<sub>4</sub>, have been computed for various dielectric media using DFT/CDM (Table 2). The Cys side chain was modeled as H<sub>2</sub>S<sup>30,34</sup> instead of CH<sub>3</sub>SH because the pK<sub>a</sub> of H<sub>2</sub>S (6.9/7.0<sup>35,36</sup>) is closer to that of Cys (8.1/8.4<sup>31,32</sup>) compared to that of CH<sub>3</sub>SH (10.3/14.2<sup>37,38</sup>).

Deprotonation of the first H<sub>2</sub>S in the tetrahedral Zn(H<sub>2</sub>S)<sub>4</sub> complex is unfavorable in the gas phase, but because of the stabilizing effect of the zinc cation on the anionic HS<sup>-</sup>, the deprotonation free energy (113 kcal/mol) is much less positive than that for the metal-free H<sub>2</sub>S (344 kcal/mol, Table 2). Due to the presence of a negatively charged ligand in the metal's first shell, ΔG<sup>1</sup> for the second deprotonation reaction increases to 205 kcal/mol even though the resulting product [Zn(H<sub>2</sub>S)<sub>2</sub>(HS<sup>-</sup>)<sub>2</sub>]<sup>0</sup> has a net zero charge. In analogy, ΔG<sup>1</sup> for deprotonating neutral [Zn(H<sub>2</sub>S)<sub>2</sub>(HS<sup>-</sup>)<sub>2</sub>]<sup>0</sup> to yield a dianionic metal [Zn(HS<sup>-</sup>)<sub>4</sub>]<sup>2-</sup> complex and two protons increases substantially (to 678 kcal/mol, Table 2) relative to the first two reactions. However, the small H<sup>+</sup> product is much better solvated than the larger metal complex reactant, thus solvation effects favor ionization. The interplay between solute electronic and solvation effects results in negative ΔG<sup>80</sup> values for all three deprotonation reactions, suggesting that the tetra-thiol zinc complex could be fully deprotonated to the corresponding tetra-thiolate species on water-exposed surfaces. Preformed solvent-inaccessible protein cavities (with ε = 2 - 4) do not seem to favor ionization of Cys-like

species, as evidenced by the large positive ΔG<sup>2</sup> and ΔG<sup>4</sup> in Table 2.

The amide backbone as well as lysine and arginine side chains, which are possible proton donors, have been found to encapsulate Cys-rich cores in zinc fingers.<sup>20</sup> Hence, the possibility of reprotonating [Zn(HS<sup>-</sup>)<sub>4</sub>]<sup>2-</sup> by a second-shell amide backbone (modeled by CH<sub>3</sub>CONHCH<sub>3</sub>) or a lysine side chain (modeled by CH<sub>3</sub>NH<sub>3</sub><sup>+</sup>) has been investigated<sup>30</sup> by computing the energies of {[Zn(HS<sup>-</sup>)<sub>4</sub>](CH<sub>3</sub>CONHCH<sub>3</sub>)<sub>2</sub>]<sup>2-</sup> and {[Zn(HS<sup>-</sup>)<sub>4</sub>](CH<sub>3</sub>NH<sub>3</sub><sup>+</sup>)<sub>2</sub>]<sup>0</sup>, and the energies of the corresponding complexes in which the amide/ammonium proton is transferred to the first-shell thiolate sulfur (see Fig. 2). The resulting electronic energies show that proton transfer from the second-shell ligand to the first-shell cysteine seems unlikely. Although the second-shell peptide backbone groups and lysine side-chains do not seem to play a role in reprotonating the first-shell cysteines, they can contribute to the stability of the Cys-rich cores, as the formation free energy of [Zn(HS<sup>-</sup>)<sub>4</sub>]<sup>2-</sup> + 2L<sup>n</sup> → ([Zn(HS<sup>-</sup>)<sub>4</sub>·L<sub>2</sub>]<sup>-2+2n</sup>) is -286 kcal/mol for L = CH<sub>3</sub>NH<sub>3</sub><sup>+</sup>, and -28 kcal/mol for L = CH<sub>3</sub>CONHCH<sub>3</sub>. These predictions are consistent with the finding that in zinc fingers the Cys-rich cores are surrounded by an elaborate network of backbone:core NH...S<sup>-</sup> hydrogen bonds, which stabilize the zinc-cysteinate structure.<sup>20</sup> Salt bridges formed between second-shell lysine or arginine side chains with first-shell cysteine have been found to additionally stabilize the binding sites in some nuclear hormone receptors, Cys- and Gly-rich proteins, polymerases and ring-finger proteins.<sup>20,39</sup>

The above results have two implications. First, in the course of metal-induced zinc finger folding, the binding of zinc to water-exposed Cys in the unfolded protein<sup>15,40,41</sup> assists the deprotonation of all the Cys. In the final folded structure, fully deprotonated Zn (Cys<sup>-</sup>)<sub>4</sub> cores, which are usually found deeply buried in the protein,<sup>30</sup> would be preserved if they are shielded from possible proton donors by hydrogen

Table 2. Calculated Deprotonation Enthalpies (ΔH<sup>1</sup>) and Free Energies (ΔG<sup>x</sup>) of Free and Metal-bound H<sub>2</sub>S for Media of Different Dielectric Constant x (in kcal/mol)<sup>a</sup>

Reaction	ΔH <sup>1,b</sup>	ΔG <sup>1</sup>	ΔG <sup>2</sup>	ΔG <sup>4</sup>	ΔG <sup>80</sup>	pK <sub>a</sub>
H <sub>2</sub> S → HS <sup>-</sup> + H <sup>+</sup>	350.5	344.1	188.9	104.9	9.1	6.7
[Zn(H <sub>2</sub> S) <sub>4</sub> ] <sup>2+</sup> → [Zn(H <sub>2</sub> S) <sub>3</sub> HS <sup>-</sup> ] <sup>+</sup> + H <sup>+</sup>	121.8	113.1	53.4	18.5	-27.7	-20.4
[Zn(H <sub>2</sub> S) <sub>3</sub> HS <sup>-</sup> ] <sup>+</sup> → [Zn(H <sub>2</sub> S) <sub>2</sub> (HS <sup>-</sup> ) <sub>2</sub> ] <sup>0</sup> + H <sup>+</sup>	210.3	204.7	107.2	53.0	-12.2	-9.0
[Zn(H <sub>2</sub> S) <sub>2</sub> (HS <sup>-</sup> ) <sub>2</sub> ] <sup>0</sup> → [Zn(HS <sup>-</sup> ) <sub>4</sub> ] <sup>2-</sup> + 2H <sup>+</sup>	692.6	678.1	354.6	181.2	-13.0	

<sup>a</sup> From Dudev & Lim, 2002;<sup>30</sup> x = 1 corresponds to gas-phase values, x = 2 or 4 represents buried or partially buried metal-binding sites, whereas x = 80 represents fully solvent-exposed sites. The experimental hydration free energy of the proton (ΔG<sub>solv</sub><sup>80</sup>(H<sup>+</sup>) = -262.5 kcal/mol) was used in computing ΔG<sup>80</sup>, while the calculated ΔG<sub>solv</sub><sup>4</sup>(H<sup>+</sup>) of -185.3 kcal/mol and ΔG<sub>solv</sub><sup>2</sup>(H<sup>+</sup>) of -119.6 kcal/mol were used in evaluating ΔG<sup>4</sup> and ΔG<sup>2</sup>, respectively. <sup>b</sup> Evaluated by MP2/6-31++G(2d,2p) calculations using fully optimized SVWN/6-31++G(2d,2p) molecular geometries.<sup>30</sup>

bonding interactions with backbone peptide groups and/or Lys/Arg side chains in the second shell.

#### D. The properties of the protein and Zn govern the specificity of the binding-site for Zn

Mg is the most abundant divalent cation in eukaryotic cells with concentrations of free Mg(II) ranging from 0.1 to 1 mM.<sup>42</sup> Zn is the second-most abundant transition metal in living organisms after iron, but its intracellular concentration is kept very low (estimated to be in the femto-molar range<sup>43</sup>) mainly by metallothionein,<sup>44</sup> a Cys-rich protein that traps up to seven Zn in its two binding domains. This raises the intriguing question of how proteins, whose natural cofactor is Zn, select this cation from the mixture of ions, especially the more abundant Mg, in the surrounding fluids? In other words, how do these proteins prevent other cations, such as Mg, from replacing Zn? It is also not clear if Zn-binding sites in proteins are generally rigid or flexible, and the extent to which the protein can adjust to the stereochemical requirements of the incoming metal ion or conversely, the metal ion can comply with the constraints of the protein matrix. To elucidate the factors governing Zn(II) selectivity by proteins the free energies of exchanging Zn for Mg in model Zn-binding sites have been computed using DFT/CDM.<sup>45</sup>

For typical *rigid* Zn-binding sites that constrain the in-

coming hexahydrated Mg to adopt the tetrahedral geometry of the outgoing Zn, Mg cannot displace Zn regardless of the solvent accessibility of the site (positive  $\Delta G_{\text{ex}}$  for first three reactions in Table 3). Even if the Zn-binding site was *flexible* and allowed Mg to adopt its preferred octahedral geometry, Mg cannot, in general, displace Zn unless one or more Asp/Glu in the outer shell could be added to the first shell of Mg in an octahedral geometry (negative  $\Delta G_{\text{ex}}$  for the last reaction in Table 3).

The finding that Mg(II) generally cannot displace Zn bound tetrahedrally to one or more histidines from Zn-binding sites (Table 3) is supported by experimental observations. Zn, the physiological activator of L-ribulose-5-phosphate 4-epimerase, binds to three histidines and, presumably, a water molecule in the protein ( $K_a = 5.9 \times 10^6 \text{ M}^{-1}$ ) more tightly than Mg ( $K_a = 7.4 \times 10^2 \text{ M}^{-1}$ ).<sup>46</sup> The same type of Zn-binding site has been proposed for the hamster dihydroorotase domain, which binds Zn, but not Mg, under physiological conditions.<sup>47</sup>

Zn can prevail over Mg in rigid buried sites as well as in flexible Zn-binding sites with *neutral* ligands in the second shell because each of the ligands transfers more charge to Zn than to Mg, thus stabilizing Zn complexes more than the corresponding Mg complexes (see section B).<sup>45,48</sup> However, Mg may displace Zn in flexible Zn-binding sites containing *nega-*

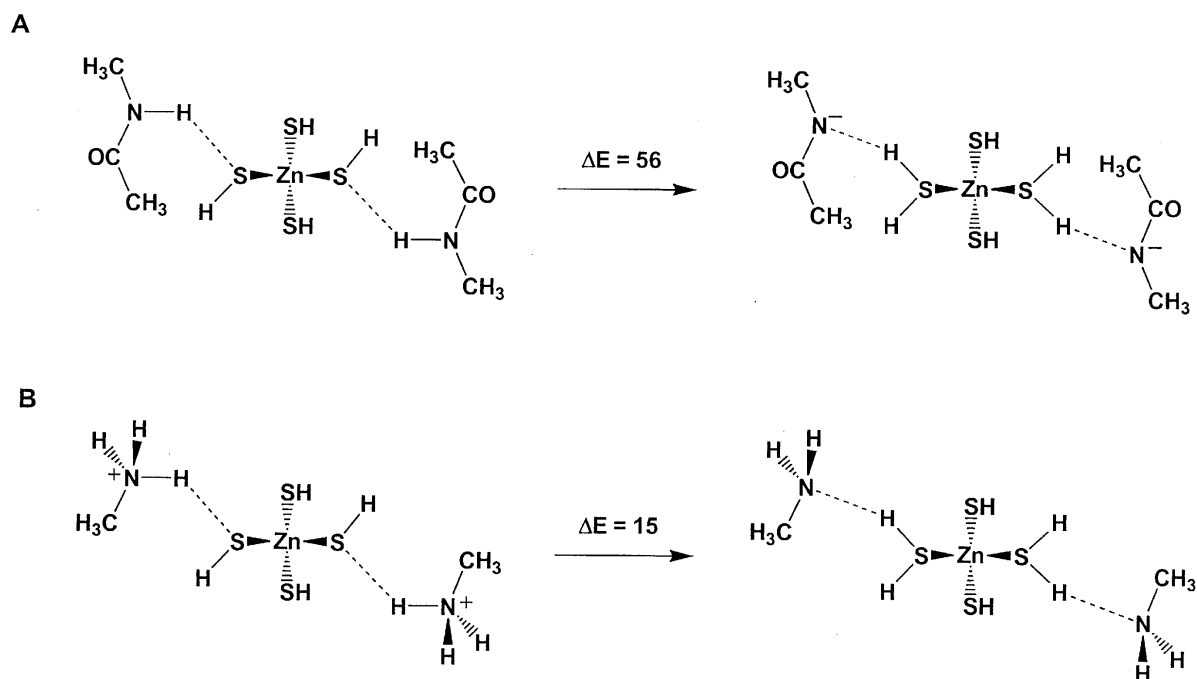


Fig. 2. Schematic diagrams of (A)  $[\text{Zn}(\text{HS}^-)_4]^{2-} \cdots 2\text{CH}_3\text{CONHCH}_3$  and  $[\text{Zn}(\text{HS}^-)_2(\text{H}_2\text{S})_2]^0 \cdots 2\text{CH}_3\text{CONCH}_3^-$ , and (B)  $[\text{Zn}(\text{HS}^-)_4]^{2-} \cdots 2\text{CH}_3\text{NH}_3^+$  and  $[\text{Zn}(\text{HS}^-)_2(\text{H}_2\text{S})_2]^0 \cdots 2\text{CH}_3\text{NH}_2$ . Isomerization energies (in kcal/mol) are taken from Dudev and Lim.<sup>30</sup>

Table 3. Enthalpies ( $\Delta H_{\text{ex}}^1$ ) and Free Energies ( $\Delta G_{\text{ex}}^x$ ) of Replacing Zn with Mg in Model Zn-binding Sites for Media of Different Dielectric Constant  $\epsilon$  (in kcal/mol)<sup>a</sup>

Reaction <sup>b</sup>	$\Delta H_{\text{ex}}^1$	$\Delta G_{\text{ex}}^1$	$\Delta G_{\text{ex}}^2$	$\Delta G_{\text{ex}}^4$	$\Delta G_{\text{ex}}^{80}$
Rigid binding sites					
$\{[\text{Zn Im W}_3] \cdot \text{W}_2\}^{2+} + [\text{Mg W}_6]^{2+} \rightarrow \{[\text{Mg Im W}_3] \cdot \text{W}_2\}^{2+} + [\text{Zn W}_6]^{2+}$	15.8 <sup>c</sup>	15.6 <sup>c</sup>	14.8	14.3	12.9
$[\text{Zn (Im)}_3 \text{ W}]^{2+} + [\text{Mg W}_6]^{2+} \rightarrow [\text{Mg (Im)}_3 \text{ W}]^{2+} + [\text{Zn W}_6]^{2+}$	29.0 <sup>c</sup>	25.7 <sup>c</sup>	25.1	24.5	23.1
$[\text{Zn (Im)}_2 (\text{CH}_3\text{S})_2]^0 + [\text{Mg W}_6]^{2+} \rightarrow [\text{Mg (Im)}_2 (\text{CH}_3\text{S})_2]^0 + [\text{Zn W}_6]^{2+}$	42.0 <sup>d</sup>	39.9 <sup>d</sup>	39.1	38.3	36.5
Flexible binding sites					
$([\text{Zn Im W}_3] \cdot \text{W}_2)^{2+} + [\text{Mg W}_6]^{2+} \rightarrow [\text{Mg Im W}_3]^{2+} + [\text{Zn W}_6]^{2+}$	14.6 <sup>c</sup>	13.9 <sup>c</sup>	8.0	4.9	0.5
$([\text{Zn Im W}_3] \cdot \text{W Fm})^{2+} + [\text{Mg W}_6]^{2+} \rightarrow [\text{Mg Im Fm W}_4]^{2+} + [\text{Zn W}_6]^{2+}$	5.2 <sup>d</sup>	6.4 <sup>d</sup>	5.0	4.5	3.7
$([\text{Zn Im W}_3] \cdot \text{W HCOO})^+ + [\text{Mg W}_6]^{2+} \rightarrow [\text{Mg Im HCOO W}_4]^+ + [\text{Zn W}_6]^{2+}$	-19.2 <sup>d</sup>	-19.3 <sup>d</sup>	-14.9	-12.4	-9.9

<sup>a</sup> From Dudev & Lim, 2001.<sup>45</sup> <sup>b</sup> Im = imidazole, W = H<sub>2</sub>O and Fm = HCONH<sub>2</sub>. <sup>c</sup> Using the 6-31++G(2d,2p) basis. <sup>d</sup> Using the 6-31+G\* basis.

tively charged but not neutral ligand(s) in the second shell (Table 3, last reaction) because the free energy gain upon Mg binding to a *negatively charged* ligand is significantly higher (by more than 200 kcal/mol) than that for Mg binding to a neutral ligand.<sup>45</sup>

The above results imply that relative to Mg, Zn has higher affinity for a given protein ligand<sup>45</sup> and strongly prefers tetrahedral geometry. Hence, a protein can generally select Zn against the background of a much higher Mg concentration. In this case, the properties of the protein (the type of metal ligands, overall charge, and shape of the cavity) and the properties of Zn (its greater charge-acceptor ability relative to Mg) govern the binding-site specificity.

#### E. Cys-rich Zn-finger cores are not well protected against heavy metals such as Cd, Hg and Pb

As discussed in the previous section, Zn-binding sites have higher specificity than corresponding Mg-binding sites, allowing the protein to sequester Zn from the cell fluids where other naturally occurring metal cofactors, such as Mg and Ca, are present. However, can these sites withstand at-

tacks by “alien” heavy metal cations such as Cd(II), Hg(II), and Pb(II), which, like Zn, prefer “soft” Cys ligands? This question has been experimentally addressed by Krizek et al.,<sup>49</sup> and, more recently, by Hartwig et al.,<sup>50-54</sup> Petering et al.,<sup>55,56</sup> Razmiafshari et al.,<sup>57</sup> and Payne et al.<sup>58</sup> In particular, Krizek and Payne have experimentally studied three small peptides (26 amino acids each) based on the consensus sequence of 131 Zn-finger domains.<sup>40</sup> The “consensus” peptides (designated as CP-CCHH, CP-CCHC, and CP-CCCC) model the three general classes of Zn-fingers and contain Cys<sub>2</sub>His<sub>2</sub>, Cys<sub>3</sub>His, and Cys<sub>4</sub> Zn-binding motifs, respectively (see Introduction). Absolute association constants ( $K_a$ ) for peptide complexes with different metal cations (Zn, Co, Cd, and Pb) have been measured in vitro by spectroscopic titration techniques, as well as  $K_a$  for other Zn-finger proteins; these are summarized in Table 4.

Despite differences in the absolute  $K_a$  numbers reported for different proteins/peptides, some general trends of changes in  $K_a$  emerge. All the binding sites in Table 4 have stronger affinity for Zn than for the other natural metal cofactor, Co ( $K_a(\text{Zn}) \gg K_a(\text{Co})$ ). Furthermore, the CP-CCHH,

Table 4. Experimental Binding Constants for Complexes between Zn-finger Domains and Divalent Metal Cations (in M<sup>-1</sup>)

Peptide/ Protein	$K_a(\text{Co})$	$K_a(\text{Zn})$	$K_a(\text{Cd})$	$K_a(\text{Pb})$
CP-CCHH	$1.6 \times 10^{7,a}$	$1.8 \times 10^{11,a}$	$5.0 \times 10^{8,a}$	$2.0 \times 10^{10,b}$
CP-CCHC	$1.6 \times 10^{7,a}$	$3.1 \times 10^{11,a}$	$1.6 \times 10^{11,a}$	$1.2 \times 10^{10,b}$
CP-CCCC	$2.8 \times 10^{6,a}$	$9.1 \times 10^{11,a}$	$2.5 \times 10^{13,a}$	$2.5 \times 10^{13,b}$
TFIIIA-CCHH <sup>c,f</sup>		$1.0 \times 10^8$	$3.6 \times 10^5$	
RMLV-CCHC <sup>d</sup>	$5.0 \times 10^7$	$1.0 \times 10^{11}$		
ERDBD-CCCC <sup>e</sup>	$1.4 \times 10^6$	$1.5 \times 10^8$	$2.1 \times 10^8$	

<sup>a</sup> From Krizek et al., 1993.<sup>49</sup> <sup>b</sup> From Payne et al., 1999.<sup>58</sup> <sup>c</sup> Transcription factor TFIIIA from Hartwig, 2001.<sup>52</sup> <sup>d</sup> Rauscher murine leukemia virus from Hartwig, 2001.<sup>52</sup> <sup>e</sup> Estrogen receptor DNA-binding domain from Hartwig, 2001.<sup>52</sup>

CP-CCHC, and TFIIIA-CCHH Zn-fingers bind Zn tighter than heavier metals such as Cd and Pb, and appear to be well protected against these metals. In contrast, the CP-CCCC and ER-CCCC Zn-fingers bind Cd and Pb tighter than Zn. Note that the  $K_a(\text{Cd})$  in the CP-series increases (by one to two orders) with each additional cysteinate ( $\text{Cys}^-$ ) in the binding site.

The above findings can be rationalized in terms of the higher affinity of the heavier and “softer” metals for  $\text{Cys}^-$  compared to Zn.<sup>49,58</sup> This is supported by *ab initio* calculations showing that Cd has higher affinity for  $\text{Cys}^-$  than Zn in octahedral and tetrahedral binding sites, whereas Zn has higher affinity for His than Cd.<sup>59</sup> Apparently, the Zn/Cd selectivity of a given binding site is governed by the relative number of Cys:His residues: the more Cys there are in the metal-binding site, the more favorable the Cd binding. Although no quantitative data on Zn-finger binding to Hg(II) have been reported so far (to the best of our knowledge), experiments on the DNA repair protein, Fpg, containing a  $\text{Cys}_4$ -binding site, and a synthetic  $\text{Cys}_2\text{His}_2$  peptide show that Hg can dislodge Zn from the respective binding sites.<sup>54,57</sup> These findings are in line with calculations predicting that the Hg dication binds  $\text{Cys}^-$  and His more favorably than Zn.<sup>59</sup>

There is growing experimental evidence that heavy metals, upon displacing Zn from the Zn-finger core, cannot maintain the proper conformation of the protein, thus disrupting the DNA-binding process.<sup>50,52-54,57,58,60,61</sup> Cd-substituted fingers, which are expected to keep the tetrahedral coordination geometry of the binding site,<sup>22</sup> cannot maintain the proper conformation of the protein probably because Cd has a larger ionic radius than Zn ( $r_{\text{Cd}} : r_{\text{Zn}} = 0.95 : 0.75 \text{ \AA}$ ), resulting in longer Cd-N(His) and Cd-S(Cys) bond distances (2.3-2.5 and 2.6  $\text{\AA}$ , respectively<sup>22</sup>) compared to the “native” Zn-N(His) and Zn-S(Cys) bond distances (2.1 and 2.3  $\text{\AA}$ , respectively<sup>13,22</sup>). Hg and Pb-bound proteins cannot maintain the proper conformation of the protein mainly because Hg and Pb prefer non-tetrahedral coordination: Hg prefers linear complexes with  $\text{Cys}^-$ ,<sup>62-64</sup> while Pb complexes are often characterized by a strongly distorted (hemidirected) coordination sphere, with the ligands occupying one half of the sphere leaving the rest of it to the metal lone pair.<sup>65</sup> Formation of mixed Zn/heavy metal complexes in the Zn-finger cores could not be ruled out.<sup>52</sup>

These studies suggest a possible mechanism for heavy metal poisoning in living cells.<sup>52,53,60</sup> Cys-rich Zn-finger cores are susceptible to attack by heavy metals. Hence, the Zn cation is ejected from the binding site by the incoming heavy metal, which cannot maintain the original fold, thus leading to Zn-finger inactivation. On the other hand, Cys-rich pro-

teins are attractive targets for toxic metals, and have been used by living organisms to fight heavy metal intoxication. Cys-rich proteins such as metallothionein are used as traps to sequester non-biogenic metals from the body fluids thus preventing the poisonous metals from damaging vital metal-binding sites.<sup>55,56,66</sup> Furthermore, evidence is increasing that metallothionein plays a role in repairing damaged Zn-binding sites by abstracting the toxic metal; e.g., Cd(II), from the binding site, and delivering the essential natural co-factor (Zn) to the same binding site.<sup>67</sup>

#### F. The outer-shell Asp/Glu carboxylate may act as a proton acceptor for the inner-shell His in solvent inaccessible Zn binding sites

PDB surveys of Zn-binding sites have shown that in about 80% of the sites a Zn-bound His is coordinated to a Asp or Glu carboxylate in the metal's second shell.<sup>12,23,68-74</sup> Experimental studies on carbonic anhydrase II and designed metal-binding sites have implicated second-shell Asp/Glu ligands in properly orienting the first-shell histidine for efficient metal binding, thus enhancing the affinity of the binding site for zinc.<sup>68,70,71,73-77</sup> To elucidate the role of this interaction, the relative energies of  $\text{ImH}\cdots\text{Ace}^-$  and  $\text{Im}^-\cdots\text{AceH}$  dyads with the distance between reaction centers fixed at either 5 or 8  $\text{\AA}$  have been calculated using *ab initio* methods, and compared with those for the respective  $\text{Zn}\cdots\text{ImH}\cdots\text{Ace}^-$  and  $\text{Zn}\cdots\text{Im}^-\cdots\text{AceH}$  triads (Fig. 3).<sup>72,78</sup> Although these energies vary with the method used and the structure of the model system, the trends of changes are the same.

In the absence of Zn the dyad  $\text{ImH}\cdots\text{Ace}^-$  is energetically more favorable than  $\text{Im}^-\cdots\text{AceH}$  (Fig. 3A), but upon Zn binding the trend reverses and  $\text{Zn}\cdots\text{Im}^-\cdots\text{AceH}$  is more stable than  $\text{Zn}\cdots\text{ImH}\cdots\text{Ace}^-$  (Fig. 3B). Indeed, when  $\text{Zn}(\text{OH})^+\cdots\text{ImH}\cdots\text{Ace}^-$  was subjected to full geometry optimization, the proton on the imidazole nitrogen migrated to acetate and formed  $\text{Zn}(\text{OH})^+\cdots\text{Im}^-\cdots\text{AceH}$  (Fig. 3C).<sup>72</sup> The same effect of proton transfer has been observed in a tetrahedral Zn complex,  $([\text{Zn}(\text{H}_2\text{O})_3\text{ImH}]\cdot(\text{H}_2\text{O})\text{HCOO})^+$ , containing an inner-sphere imidazole hydrogen-bonded to an outer-sphere formate so that the final fully optimized structure was a Zn-bound imidazolate anion hydrogen bonded to formic acid (Fig. 3D).<sup>45</sup>

In the absence of Zn,  $\text{ImH}\cdots\text{Ace}^-$  is energetically preferred over  $\text{Im}^-\cdots\text{AceH}$  because the proton dissociation energy of ImH is slightly more positive than that of AceH (349 vs. 345 kcal/mol; B3LYP/6-311+G(d,p) calculations).<sup>78</sup> However, upon Zn binding the gas-phase proton dissociation energy of ImH drops significantly (to 117 kcal/mol)<sup>78</sup> due to stabilization of the negatively charged imidazolate anion by

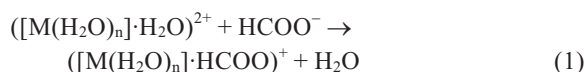
the metal dication through charge-charge interactions and charge-transfer from the imidazolate to the metal. Furthermore, in a solvent-inaccessible cavity charge-charge-dipole electrostatic interactions in  $\text{Zn}\cdots\text{Im}^-\cdots\text{AceH}$  would be much more favorable than the charge-dipole-charge interactions in  $\text{Zn}\cdots\text{ImH}\cdots\text{Ace}^-$ .

These findings in conjunction with earlier results reported by Krauss and Garmer<sup>69</sup> imply that Asp/Glu may act as a *proton acceptor* for the Zn-bound-His rather than as a hy-

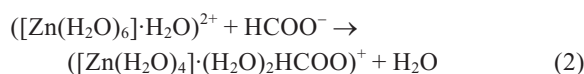
drogen bonding partner if the metal-binding site is solvent-inaccessible, and the deprotonated/protonated Asp/Glu is not strongly stabilized/destabilized by other protein interactions, respectively. This in turn implies an important role of the second coordination layer in metal binding to proteins.

### G. Second-shell ligands may contribute to the specificity of the metal binding site

Although the metal specificity of a given binding site is primarily determined by the structure and properties of its first coordination layer (see above, sections D and E), it is not clear if the outer shell contributes to the metal specificity of a given binding site, and if so, to what extent. To address these questions DFT/CDM<sup>23</sup> has been used to compute the free energies of replacing a second-shell water with formate (representing the deprotonated Asp or Glu side chain), which is modeled as:



or in the case of Zn, which prefers to be tetra-coordinated in proteins (see section B), as



where the Zn coordination number in the product is four with two water molecules and a formate in the outer shell. In eqs 1 and 2, the number of water molecules in the first shell,  $n$ , is six for  $\text{M} = \text{Mg}^{2+}$ ,  $\text{Mn}^{2+}$ , or  $\text{Zn}^{2+}$ , and seven for  $\text{Ca}^{2+}$ .

Due to the strong electrostatic interaction between the negatively charged formate and the positively charged metal-hydrate the  $\Delta G^x$  ( $x = 1, 2$  or  $4$ ) is large and negative (Table 5), implying that 2<sup>nd</sup>-shell water-formate exchange is favorable in both the gas phase and in a buried or partially buried cavity. However, it does not appear to be sensitive to metal cations with the same coordination geometry and similar ionic radii:  $\Delta G^x$  ( $x = 1, 2, 4$ ) for the octahedral complexes of Mg, Zn, and Mn, whose ionic radii are 0.72, 0.75, and 0.83 Å, respectively,<sup>24</sup> differ by only 1-3 kcal/mol. Decreasing the Zn coordination number from six to four results in an additional free energy gain (of 5-9 kcal/mol, compare reactions 3 and 4 in Table 5). The *heptacoordinated* Ca complexes have the smallest absolute exchange free energies in the series (last reaction in Table 5): the  $|\Delta G^x|$  values ( $x = 1, 2$  or  $4$ ) are smaller than those for the *hexacoordinated* Mg, Mn, and Zn complexes (by 6-14 kcal/mol) and are much smaller than those for the *tetracoordinated* Zn complex (by 13-23 kcal/mol).

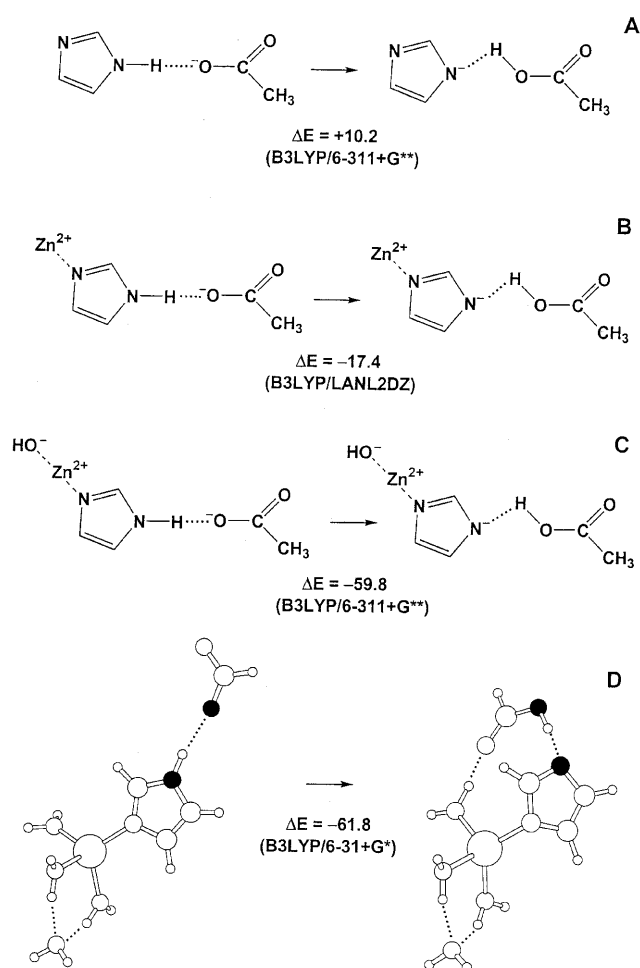


Fig. 3. Schematic diagrams of (A)  $\text{ImH}\cdots\text{Ace}^-$  and  $\text{Im}^-\cdots\text{AceH}$ , (B)  $\text{Zn}\cdots\text{ImH}\cdots\text{Ace}^-$  and  $\text{Zn}\cdots\text{Im}^-\cdots\text{AceH}$ , (C)  $\text{Zn}(\text{OH})^+\cdots\text{ImH}\cdots\text{Ace}^-$  and  $\text{Zn}(\text{OH})^+\cdots\text{Im}^-\cdots\text{AceH}$ . (D) Initial structure of  $[\text{Zn}\cdots\text{ImH}\cdots(\text{H}_2\text{O})_3 \cdot \text{HCOO}^- \cdot \text{H}_2\text{O}]^+$  and the final fully optimized structure  $[\text{Zn}\cdots\text{Im}^-\cdots(\text{H}_2\text{O})_3 \cdot \text{HCOOH} \cdot \text{H}_2\text{O}]^+$ . Isomerization energies (in kcal/mol) computed at a given theory/basis level (in brackets) are listed below the respective structures. The distance between reaction centers in (A), (B), and (C) has been fixed at 5 Å.

Table 5. Enthalpies ( $\Delta H^1$ ) and Free Energies ( $\Delta G^x$ ) (in kcal/mol) of Water-formate Exchange for Media of Different Dielectric Constant  $x^a$ 

Reaction	$\Delta H^{1,b}$	$\Delta G^{1,b}$	$\Delta G^2$	$\Delta G^4$
$([\text{Mg}(\text{H}_2\text{O})_6 \cdot \text{H}_2\text{O}]^{2+} + \text{HCOO}^- \rightarrow ([\text{Mg}(\text{H}_2\text{O})_6] \cdot \text{HCOO})^+ + \text{H}_2\text{O}$	-188.0	-183.2	-85.4	-36.6
$([\text{Mn}(\text{H}_2\text{O})_6 \cdot \text{H}_2\text{O}]^{2+} + \text{HCOO}^- \rightarrow ([\text{Mn}(\text{H}_2\text{O})_6] \cdot \text{HCOO})^+ + \text{H}_2\text{O}$	-186.6	-182.2	-84.0	-35.0
$([\text{Zn}(\text{H}_2\text{O})_6 \cdot \text{H}_2\text{O}]^{2+} + \text{HCOO}^- \rightarrow ([\text{Zn}(\text{H}_2\text{O})_6] \cdot \text{HCOO})^+ + \text{H}_2\text{O}$	-190.0	-185.2	-86.2	-36.8
$([\text{Zn}(\text{H}_2\text{O})_6 \cdot \text{H}_2\text{O}]^{2+} + \text{HCOO}^- \rightarrow ([\text{Zn}(\text{H}_2\text{O})_4] \cdot (\text{H}_2\text{O})_2 \cdot \text{HCOO})^+ + \text{H}_2\text{O}$	-195.4	-193.9	-92.5	-41.7
$([\text{Ca}(\text{H}_2\text{O})_7 \cdot \text{H}_2\text{O}]^{2+} + \text{HCOO}^- \rightarrow ([\text{Ca}(\text{H}_2\text{O})_7] \cdot \text{HCOO})^+ + \text{H}_2\text{O}$	-176.2	-171.2	-76.5	-28.7

<sup>a</sup> From Dudev et al., 2002.<sup>23</sup> <sup>b</sup> Evaluated by employing B3LYP/6-31++G(2d,2p) calculations.

The reason why exchanging an outer-shell water molecule for a formate becomes less favorable with increasing coordination number of the core metal can be understood in terms of charge-charge, charge-dipole, and charge-transfer interactions, which make the major contributions to the metal complex stability. Increasing the coordination number of the complex results in an increase in the metal-2<sup>nd</sup>-shell-ligand distance, which, in turn, leads to a weakening of the charge-charge and charge-dipole interactions. This, together with the decreasing formate-metal charge transfer and increasing steric repulsion among the ligands with increasing metal coordination number largely accounts for the observed decrease in the  $|\Delta H^1|$  (Table 5) with increasing metal coordination number.

The results obtained imply that first-second-shell interactions in metal-binding sites may be discriminative toward dications possessing different coordination geometries. In this way the outer layer appears to contribute to the metal specificity and selectivity of the binding site. The 2<sup>nd</sup> shell favors cations such as Zn that prefer tetrahedral to octahedral geometry and that can successfully compete with bulkier cations with seven or more inner-shell ligands for the binding site, but it is much less discriminative toward metal ions with the same coordination geometry and similar ionic size, such as octahedral Mg, Mn and Zn (Table 5). Indirect support for the ability of 2<sup>nd</sup>-shell ligands to discriminate between metal dications with different coordination geometry comes from the works of Karlin and associates who have shown that the structure of the second shell depends on, and thus appears to be specific to, the type of the bound metal.<sup>79-81</sup>

## ACKNOWLEDGMENTS

T.D. is supported by the Institute of Biomedical Sciences. This work is supported by the Institute of Biomedical Sciences at Academia Sinica, the National Center for High Performance Computing, and the National Science Council,

Republic of China (NSC-91-2113-M-001-043).

Received January 2, 2003.

## REFERENCES

- Thomson, A. J.; Gray, H. B. *Curr. Opin. Struct. Biol.* **1998**, *2*, 155.
- Frausto da Silva, J. J. R.; Williams, R. J. P. *The biological chemistry of the elements*; Oxford University Press: Oxford, 1991.
- Bertini, I.; Gray, H. B.; Lippard, S. J.; Valentine, J. S. *Bioinorganic Chemistry*; University Science Books: Mill Valley, California, 1994.
- Bertini, I.; Sigel, A.; Sigel, H., Eds. *Handbook on Metalloproteins*; Marcel Dekker: New York, 2001.
- Lippard, S. J.; Berg, J. M. *Principles of Bioinorganic Chemistry*; University Science Books: Mill Valley, California, 1994.
- Yamashita, M. M.; Wesson, L.; Eisenman, G.; Eisenberg, D. *Proc. Natl. Acad. Sci. USA* **1990**, *87*, 5648.
- Dudev, T.; Lim, C. *J. Phys. Chem. B* **2000**, *104*, 3692.
- Sun, G.; Budde, R. J. A. *Biochemistry* **1999**, *38*, 5659.
- Vallee, B. L.; Auld, D. S. *Biochemistry* **1990**, *29*, 5647.
- Christianson, D. W. *Adv. Prot. Chem.* **1991**, *42*, 281.
- Coleman, J. E. *Annu. Rev. Biochem.* **1992**, *61*, 897.
- Lipscomb, W. N.; Strater, N. *Chem. Rev.* **1996**, *96*, 2375.
- Alberts, I. L.; Nadassy, K.; Wodak, S. J. *Prot. Sci.* **1998**, *7*, 1700.
- Christianson, D. W.; Cox, J. D. *Annu. Rev. Biochem.* **1999**, *68*, 33.
- Berg, J. M.; Godwin, H. A. *Annu. Rev. Biophys. Biomol. Struct.* **1997**, *26*, 357.
- Hanas, J. S.; Hazuda, D. J.; Bogenhagen, D. F.; Wu, F. Y.-H.; Wu, C.-W. *J. Biol. Chem.* **1983**, *258*, 14120.
- Miller, J.; McLachlan, A. D.; Klug, A. *EMBO J.* **1985**, *4*, 1609.
- Summers, M. F.; South, T. L.; Kim, B.; Hare, D. *Biochemistry* **1990**, *29*, 329.
- Petkovich, M.; Brand, N. J.; Krust, A.; Chambon, P. *Nature*

- 1987, 330, 444.
20. Maynard, A. T.; Covell, D. G. *J. Am. Chem. Soc.* **2001**, *123*, 1047.
21. Jernigan, R.; Raghunathan, G.; Bahar, I. *Curr. Op. Struct. Biol.* **1994**, *4*, 256.
22. Rulisek, L.; Vondrasek, J. *J. Inorg. Biochem.* **1998**, *71*, 115.
23. Dudev, T.; Lin, Y. L.; Dudev, M.; Lim, C. *J. Am. Chem. Soc.* **2003**, *125*, 3168.
24. Marcus, Y. *Chem. Rev.* **1988**, *88*, 1475.
25. Ryde, U. *Biophys. J.* **1999**, *77*, 2777.
26. Bock, C. W.; Katz, A. K.; Markham, G. D.; Glusker, J. P. *J. Am. Chem. Soc.* **1999**, *121*, 7360.
27. Dudev, T.; Lim, C. *J. Am. Chem. Soc.* **2000**, *122*, 11146.
28. Ryde, U. *J. Comp. Aided Mol. Des.* **1996**, *10*, 153.
29. Ryde, U. *Proteins: Struct. Func. Genet.* **1995**, *21*, 40.
30. Dudev, T.; Lim, C. *J. Am. Chem. Soc.* **2002**, *124*, 6759.
31. Dawson, R. M. C.; Elliot, D. C.; Elliot, W. H.; Jones, K. M. *Data for Biochemical Research*; 3rd ed.; Clarendon Press: Oxford, 1995.
32. Lide, D. R., Ed. *Handbook of Chemistry and Physics*; CRC Press: Boca Raton, 1998.
33. Hightower, K. E.; Huang, C.-C.; Casey, P. J.; Fierke, C. A. *Biochemistry* **1998**, *37*, 15555.
34. Dudev, T.; Lim, C. *J. Phys. Chem. B* **2001**, *105*, 10709.
35. Pearson, R. G. *J. Am. Chem. Soc.* **1986**, *108*, 6109.
36. Atkins, P. W. *Physical Chemistry*; Sixth edition; Oxford University Press: Oxford, 1999.
37. Howard, P. H.; Meylan, W. M., Eds. *Handbook of Physical Properties of Organic Chemicals*; Lewis Publishers: Boca Raton, 1997.
38. Irving, R. J.; Nelender, L.; Wadso, I. *Acta Chem. Scand.* **1964**, *18*, 769.
39. Konrat, R.; Weiskirchen, R.; Bister, K.; Krautler, B. *J. Am. Chem. Soc.* **1998**, *120*, 7127.
40. Krizek, B. A.; Amann, B. T.; Kilfoil, V. J.; Merkle, D. L.; Berg, J. M. *J. Am. Chem. Soc.* **1991**, *113*, 4518.
41. Miura, T.; Satoh, T.; Takeuchi, H. *Biochim. Biophys. Acta* **1998**, *1384*, 171.
42. Romani, A.; Scarpa, A. *Arch. Biochem. Biophys.* **1992**, *298*, 1.
43. Suhy, D. A.; Simon, K. D.; Linzer, D. I. H.; O'Halloran, T. V. *J. Biol. Chem.* **1999**, *274*, 9183.
44. Maret, W. *Proc. Natl. Acad. Sci. USA* **1994**, *91*, 237.
45. Dudev, T.; Lim, C. *J. Phys. Chem. B* **2001**, *105*, 4446.
46. Lee, L. V.; Poyner, R. R.; Vu, M. V.; Cleland, W. W. *Biochemistry* **2000**, *39*, 4821.
47. Huang, D. T. C.; Thomas, M. A. W.; Christopherson, R. I. *Biochemistry* **1999**, *38*, 9964.
48. Garmer, D. R.; Gresh, N. *J. Am. Chem. Soc.* **1994**, *116*, 3556.
49. Krizek, B. A.; Merkle, D. L.; Berg, J. M. *Inorg. Chem.* **1993**, *32*, 937.
50. Hartwig, A. *Toxicol. Lett.* **1998**, *102-103*, 235.
51. Hartwig, A. *Pure Appl. Chem.* **2000**, *72*, 1007.
52. Hartwig, A. *Antiox. Redox Signaling* **2001**, *3*, 625.
53. Hartwig, A.; Asmuss, M.; Blessing, H.; Hoffmann, S.; Jahnke, G.; Khandelwal, S.; Polzer, A.; Burkle, A. *Food Chem. Toxicol.* **2002**, *40*, 1179.
54. Asmuss, M.; Mullenders, L. H. F.; Hartwig, A. *Toxicol. Lett.* **2000**, *112-113*, 227.
55. Petering, D. H.; Huang, M.; Moteki, S.; Shaw III, C. F. *Marine Environ. Res.* **2000**, *50*, 89.
56. Moteki, S. A.; Huang, M.; Shaw III, C. F.; Petering, D. H. *J. Inorg. Biochem.* **1999**, *74*, 239.
57. Razmiafshari, M.; Kao, J.; d'Avignon, A.; Zawia, N. H. *Toxicol. Appl. Pharmacol.* **2001**, *172*, 1.
58. Payne, J. C.; Horst, M. A. T.; Godwin, H. A. *J. Am. Chem. Soc.* **1999**, *121*, 6850.
59. Rulisek, L.; Havlas, Z. *J. Am. Chem. Soc.* **2000**, *122*, 10428.
60. Predki, P. F.; Sarkar, B. *J. Biol. Chem.* **1992**, *267*, 5842.
61. Sarkar, B. *Nutrition* **1995**, *11*, 646.
62. Yamamura, T.; Watanabe, T.; Kikuchi, A.; Yamane, T.; Ushiyama, M.; Hirota, H. *Inorg. Chem.* **1997**, *36*, 4849.
63. DeSilva, T. M.; Veglia, G.; Porcelli, F.; Prantner, A. M.; Opella, S. J. *Biopolymers* **2002**, *64*, 189.
64. Matzapetakis, M.; Farrer, B. T.; Weng, T.-C.; Hemmingsen, L.; Penner-Hahn, J. E.; Pecoraro, V. L. *J. Am. Chem. Soc.* **2002**, *124*, 8042.
65. Shimony-Livny, L.; Glusker, J. P.; Bock, C. W. *Inorg. Chem.* **1998**, *37*, 1853.
66. Huan, Y.; Chu, D. Y.; Tang, Y.; Cao, W. *Acta Phys. Chim. Sinica* **2000**, *16*, 764.
67. Roesijadi, G. *Cell. Mol. Biol.* **2000**, *46*, 393.
68. Christianson, D. W.; Alexander, R. S. *J. Am. Chem. Soc.* **1989**, *111*, 6412.
69. Krauss, M.; Garmer, D. R. *J. Am. Chem. Soc.* **1991**, *113*, 642.
70. Lesburg, C. A.; Christianson, D. W. *J. Am. Chem. Soc.* **1995**, *117*, 6838.
71. Kiefer, L. L.; Paterno, S. A.; Fierke, C. A. *J. Am. Chem. Soc.* **1995**, *117*, 6831.
72. El Yazal, J.; Roe, R. R.; Pang, Y.-P. *J. Phys. Chem. B* **2000**, *104*, 6662.
73. Cox, E. H.; Hunt, J. A.; Compher, K. M.; Fierke, C. A.; Christianson, D. W. *Biochemistry* **2000**, *39*, 13687.
74. McCall, K. A.; Huang, C.-C.; Fierke, C. A. *J. Nutr.* **2000**, *130*, 1437S.
75. Huang, C.-C.; Lesburg, C. A.; Kiefer, L. L.; Fierke, C. A.; Christianson, D. W. *Biochemistry* **1996**, *35*, 3439.
76. Marino, S. F.; Regan, L. *Chem. & Biol.* **1999**, *6*, 649.
77. DiTusa, C. A.; McCall, K. A.; Christensen, T.; Mahapatro, M.; Fierke, C. A.; Toone, E. J. *Biochemistry* **2001**, *40*, 5345.
78. El Yazal, J.; Pang, Y.-P. *J. Phys. Chem. B* **1999**, *103*, 8773.
79. Karlin, S.; Zhu, Z.-Y. *Proc. Natl. Acad. Sci. USA* **1997**, *94*, 14231.
80. Karlin, S.; Zhu, Z.-Y.; Karlin, K. D. *Proc. Natl. Acad. Sci. USA* **1997**, *94*, 14225.
81. Karlin, K. D.; Zhu, Z.-Y.; Karlin, S. *J. Biol. Inorg. Chem.* **1998**, *3*, 172.